






Analysis of Weight-Directed Functional Brain Networks in the Deception State Based on EEG Signal

Sihong Wei, Junfeng Gao , Yong Yang, Neal Xiong , Jiaqi Zhang , Jian Song , Qianruo Kang ,
Yaqian Li, and Haoan Lv

Abstract—Although analyzing the brain’s functional and structural network has revealed that numerous brain networks are necessary to collaborate during deception, the directionality of these functional networks is still unknown. This study investigated the effective connectivity of the brain networks during deception and uncovers the information-interaction patterns of lying neural oscillations. The electroencephalography (EEG) data of 40 lying persons and 40 honest persons were used to create the weight-directed functional brain networks (WDFBN). Specifically, the connecting edge weight was defined based on the normalized phase transfer entropy (dPTE) between each electrode pair, where the network nodes involved 30 electrode channels. Additionally, the signal connectivity matrices were constructed in four frequency bands: delta, theta, alpha, and beta and were subjected to a difference analysis of entropy values between the groups. Statistical analysis of the classification results revealed that all frequency bands correctly detect deception and innocence with an accuracy of 92.83%, 94.17%, 85.93%, and 92.25%, respectively. Therefore, dPTE can be considered a valuable feature for identifying lying. According to WDFBN analysis, deception has stronger information flow in the frontoparietal, frontotemporal and temporoparietal networks compare to honest

people. Furthermore, the prefrontal cortex was also found to be activated in all frequency ranges. This study examined the critical pathways of brain information interaction during deception, providing new insights into the underlying neural mechanisms. Our analysis offers significant evidence for the development of brain networks that could potentially be used for lie detection.

Index Terms—Deception detection, effective connectivity, electroencephalography (EEG), normalized phase transfer entropy (dPTE), weight-directed functional brain networks (WDFBN).

I. INTRODUCTION

A WHITE lie is not malicious or profitable and is mindful of others. However, some lies are said to conceal the truth for personal advantage and advancement, which is known as deception [1]. Deception detection is an essential scientific issue investigating the psychological and physiological changes that occur when people lie. Specialists have worked hard to develop effective approaches to detecting lies [2], [3], [4]. Although polygraph detection’s authenticity and validity are debatable, it is crucial in criminal investigations, airport security, anti-terrorism, and other domains [5]. The polygraph study examined the subject’s verbal and nonverbal activities [6] and a multichannel polygraph technology was devised to detect participants’ physiological signs like blood pressure, pulse, and skin electricity [7]. Various studies indicate that the nature of lying is a complex cognitive process involving the transmission of information between neurons in different brain regions [8], [9]. It is difficult to accurately distinguish the differences between the honesty group and the lying group solely based on physiological indicators.

A recent advance in lie detection investigates the distinct components of event-related potentials (ERP) based on brain cognition [10]. Unlike a multichannel polygraph, ERP does not detect physiological signs of the human body but instead analyzes real-time functional changes in the human brain. Through superposition technology, Picton et al. found the P300 [11] component of endogenous evoked potentials induced by rare stimuli for the first time and illustrated that this ERP component is related to memory and thinking and reflects the brain’s cognitive processing [12]. According to a significant number of research

Manuscript received 21 November 2022; revised 20 March 2023; accepted 9 July 2023. Date of publication 17 July 2023; date of current version 5 October 2023. This work was supported by the National Natural Science Foundation of China under Grant 61773408. (Sihong Wei and Yong Yang contributed equally to this work) (Corresponding authors: Junfeng Gao; Jian Song.)

This work involved human subjects or animals in its research. Approval of all ethical and experimental procedures and protocols was granted by the Cognitive Neuroscience Research Committee of South-central Minzu University. (Followed the World Medical Association’s Declaration of Helsinki for medical research involving humans.)

Sihong Wei, Junfeng Gao, Jiaqi Zhang, Qianruo Kang, Yaqian Li, and Haoan Lv are with the Key Laboratory of Cognitive Science of State Ethnic Affairs Commission, Hubei Key Laboratory of Medical Information Analysis and Tumor Diagnosis and Treatment, College of Biomedical Engineering, South-Central Minzu University, Wuhan 430074, China (e-mail: wsh_cathy@163.com; junfengmst@163.com; jiaqizhang_work@163.com; kang_980214@163.com; lyqdyxy@126.com; lvhaoan0528@163.com).

Yong Yang is with the School of Computer Science and Technology, Tiangong University, Tianjin 300387, China (e-mail: greatyangy@126.com).

Neal Xiong is with the Department of Computer Science, Georgia State University, Atlanta, GA 30302 USA (e-mail: xiong31@nsuok.edu).

Jian Song is with the Department of Neurosurgery, General Hospital of the Central Command Theater of PLA, Wuhan 430070, China (e-mail: songjian0505@smu.edu.com).

Digital Object Identifier 10.1109/JBHI.2023.3295892

findings, the P300 components are more likely to be induced by familiar objects than new things [13], where the amplitude of P300 is higher [14]. However, the results of Labkovsky et al. [15] demonstrated that the false positive rate of deception detection utilizing P300 remains significant. Based on this, researchers used nonlinear analysis techniques to extract features from multi-channel ERP and machine learning to identify and classify features, which not only facilitates further decoding of the information processing mechanism of the brain during deception, but also further improves the accuracy of deception detection [2], [16], [17].

Numerous research works highlight that neural mechanisms inherent in lying are different from truth-telling [18], [19]. Lying may cause increased activity in critical loop of brain, leading to changes in conflict and attention distribution [20], [21]. This is because executing lying behavior requires more attention to control language and behavior to produce stronger memory and attention focus. These changes can be detected using techniques such as electroencephalography (EEG), functional magnetic resonance imaging (fMRI) and functional near-infrared spectroscopy (fNIRS) technology and serve as a basis for detecting deception. In 2013, Ding et al. [22] used fNIRS to explore the neural responses of spontaneous deception and found that the left superior frontal gyrus was involved in indicative deception. They pointed out that lying involves more cognitive processes as it requires simultaneous working memory and task switching. Li et al. [23] conducted a study on deception using EEG and found that intentional deception caused smaller P300 and larger N200 compared to the honesty group during the decision-making stage. They also confirmed that deception involves executive control processes. Yu et al. [24] used fMRI to explore the neural mechanisms underlying deception and false memory and found that the deception task was associated with enhanced activation in the right superior frontal gyrus, right superior temporal gyrus, and left inferior parietal lobule. Their research results demonstrated that executive control processes, especially working memory, play an essential role in deception. Compared with fMRI and fNIRS, EEG has a millisecond-level time resolution, easy collection and low-cost advantages. Considering that the frequency components of signals are functionally related to information processing, we choose to use EEG, which is more focused on brain neural oscillations, to study the neural mechanisms of lying.

Since the cognitive processing of deception involves moving from motivation generation to cognitive decision-making and constructing an action response [25], [26], research should not only focus on the brain regions activated during lying, but also on the functional connections between different brain regions. Various studies have demonstrated that brain networks can be used to investigate the structural and functional relationships between distinct brain regions. Brain network theory has been used to examine brain mechanics as well as other cognitive processes like emotion recognition, motor imagery, and language processing [27], [28], [29], offering a comprehensive perspective on EEG-based deception detection. Previous works indicated that neural circuits established by brain regions such as the anterior cingulate cortex, superior frontal cortex, anterior

parietal cortex, premotor and motor cortex, and premotor and motor cortex comprise a crucial brain network system for deception [17], [30]. Numerous studies constructed the structural and functional brain network applying nonlinear interdependence because EEG signals have typical non-stationary characteristics [31], [32], [33]. The study of EEG has revealed that the connectivity between the upper and middle frontal gyrus in the left hemisphere is enhanced during lying [34]. Another study used cross-coherence, phase synchronization, and mutual information nonlinear feature extraction methods to compare different functional connectives. The results revealed that the brain network under deception has a “small world” quality and that the functional connections between the two subjects in the frontal, central, and parietal areas are significantly different [21]. Those studies demonstrated that functional connectivity patterns induced by a deception task differ from those induced by honest behavior, and brain network features are extracted and applied in a pattern recognition polygraph system on multichannel EEG signals, improving lie detection accuracy.

Although EEG has been used to decode the whole brain’s functional connectivity for deception purposes, the directionality of these connections in large-scale functional networks remains unknown. The human brain system is so complicated that investigating the direction of the information flow across brain areas can reveal more about the deception’s brain neural activity mechanism [35]. Therefore, it is necessary to use an effective connectivity method that can analyze the direct causal influence of one brain region on another. Phase transfer entropy (PTE) is a causal nonlinear analysis method based on information theory, which can assess the direction of information transfer in real-time between two time series, and has the advantages of accuracy, interpretability, and handling asymmetric data [36]. Although a similar approach is used in the study of Alzheimer’s disease and major depressive disorder [35], [37], [38], there has been no research employing PTE to investigate the effective connectivity of the brain during deception.

To reveal the interactive relationship between brain regions on four sub-bands (delta, theta, beta, and alpha) during deception, this study constructed weight-directed functional brain networks (WDFBN) based on EEG by normalized phase transfer entropy (dPTE) [37]. To explore the ability of extracted network features in deception detection, the dPTE features obtained from four sub-bands were inputted into CatBoost, linear regression (LR), and support vector machine (SVM) classifiers, respectively. Eventually, the information flow patterns of the human brain in deception and honesty states were analyzed based on the statistics and classification results, and the neural activity mechanism of lying in the four sub-bands were analyzed in detail according to the differences between the two patterns. This research aims to evaluate the feasibility of the proposed unique approach by utilizing an EEG-based lab deception detection experiment. The remainder of this article is organized as follows: Section II describes the experimental protocol and methodology, presents the employed data preprocessing, uses dPTE as the feature extraction method, and conducts statistical tests and classification analysis. Section III presents the performance analysis results,

and Section IV discusses the corresponding results. Finally, Section V concludes this work.

II. MATERIALS AND METHODS

A. Subjects

This study involved 80 healthy university students (Male/Female: 48/32, Mean age: 19.6 ± 4.8 years old), all right-handed, with normal vision and hearing, and no history of psychological disorders. The subjects (students) were randomly assigned to one of two groups: honesty or lying. The honesty group served as the experimental control group, allowing researchers to investigate the specific information interaction patterns in brain areas during the deception. When the Wilcoxon rank-sum test was used to compare the honesty and deception groups, the p-values for gender ($p = 0.25$) and age ($p = 0.32$) suggested no significant difference between the two groups. The subjects had to refrain from drinking, smoking, and taking any medicine for four hours before the deception detection. Before the experiment, the researchers double-checked that the participants were free of symptoms such as cough, cold, or fever. The goal of this experiment and the complete protocol was explained to all participants, who then signed an informed permission form. The Cognitive Neuroscience Research Committee of the School of Biomedical Engineering, South-Central Minzu University, examined and approved the study, which followed the ethical norms of the World Medical Association's Declaration of Helsinki for medical research involving humans.

B. Experimental Protocol and Task

Participants had to undertake a simulated crime scenario and then made a dishonest or honest response in a subsequent lie test to analyze the functional connections pattern of neural oscillations in the brain during deception. This study adopted Farwell and Donchin's three-stimulus experimental model for the Guilty Knowledge Test (GKT) [39]. GKT is a method for detecting a priori knowledge of crime scene details using psychophysiological means, and it is frequently used to determine if someone is lying about something. In GKT, subjects are typically exposed to three stimulus categories: 1) Probe stimulus (P): linked to a concealed message that only the guilty subjects are aware of. 2) Target stimuli (T): unrelated to the hidden message, where all participants are familiar with them and responsible for attracting the subject's attention during the GKT. 3) Irrelevant stimuli (I): this stimulus was unknown to all subjects and was irrelevant to the hidden message. Fig. 1 illustrates the experimental protocol design flow based on the principles of the GKT experimental paradigm.

The researcher prepared two safes (#1 and #2), six bracelets, and an image corresponding to each bracelet. For the deception group, the researcher placed two selected bracelets in safe #2 and designated the remaining four bracelets as I stimuli. The experiment required subjects to take two bracelets prepared from the safe and, after carefully observing the shape, color, size, and other information about the bracelets' appearance, randomly select one to be stolen and informed the experimental researcher,

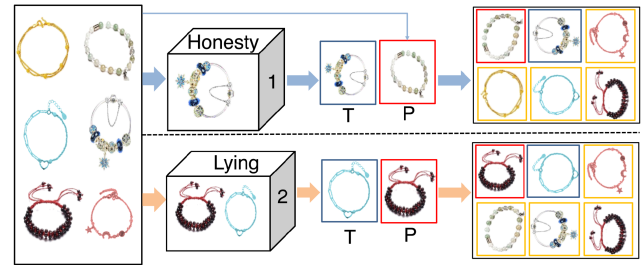


Fig. 1. Experimental protocol. Prior to the start of the experiment, subjects were required to observe or steal the bracelet. P, T, and I stimuli were shown in red, blue and yellow rectangle, respectively.

who then labeled the bracelet to be stolen by the subject as P stimuli and the other bracelet as T stimuli. For the innocent group, one bracelet was selected and placed in safe #1 and marked as T stimuli, another bracelet was randomly selected and marked as P stimuli, and the remaining four bracelets were marked as I stimuli. The honest people had to take the only bracelet from the safe and record the information about the bracelet's appearance in terms of color, shape, and size. All stimuli (bracelet pictures) were edited and controlled in a pseudo-random sequence using software (E-prime, 2.0) so that six different bracelet pictures appeared on the computer screen a total of 30 times during each experiment, with the P stimuli appearing 5 times (16.7%), the T stimuli appearing 5 times (16.7%), and the I stimuli appearing 20 times (66.7%).

Following the above setup, the subjects were instructed to sit in a chair one meter away from the computer screen, focus on the computer screen during the experiment, and finish the task with their eyes in the center of the screen. It is worth noting that the head could not move freely during the operation, the number of blinks should be kept to a minimum, and the hands should only be used to click the mouse. During the task, the "+" sign appeared for 0.3 s before the bracelet (stimulus) picture appeared, reminding the subject that the stimulus would appear soon and to focus on it. Immediately after, the stimulus picture appeared and stayed for 0.5 s, followed by the line "Have you seen this bracelet?" for 0.5 s, and the participant had to respond as quickly and accurately as possible by clicking the mouse (Fig. 2(a) Experimental task). If the subject had seen the bracelet, he clicked the left (L) mouse button (Yes). Otherwise, click the right (R) mouse button (No). When the P and I stimuli appeared on the computer screen, the subject clicked the R mouse button, and when the T stimulus occurred, the subject pressed the L mouse button (Fig. 2(a) EEG recording). Thus, the deceiver had only to lie in response to the P stimulus, while the honest person had to act honestly in all situations. Each participant completed 10 experiments. Each trial lasted 1.6 s, and each experiment was separated by five minutes. Before the experimental start, all subjects were trained in the test to attain a click accuracy of at least 95%.

C. EEG Recording and Preprocessing

The EEG cap has 64 standard scalp electrodes conforming to the International 10-10 system. The EEG data were recorded

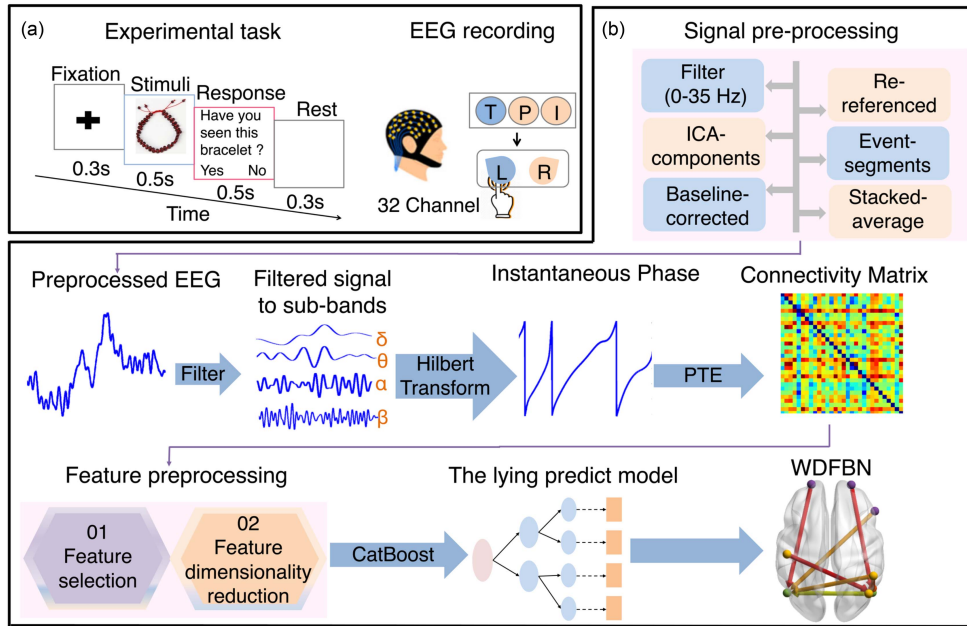


Fig. 2. Methodology overview. (a) Experimental procedure. (b) The schematic procedure of WDFBN of the EEG signal. PTE represents computing the connectivity matrix of the signal using the phase transfer entropy algorithm. WDFBN: weight-directed functional brain networks.

using a 32-channel Synamps amplifier. The sampling frequency was 500 Hz, and the lead impedance was less than 5 k Ω . The participant was given a few minutes to relax with their eyes closed until they confirmed they were ready to start the experiment, after which their EEG signal was recorded for five minutes at rest. Furthermore, EEG raw data from the subject's lie detection experiment was collected. The EEG data were preprocessed using the EEGLAB toolkit. Specifically, a band-pass filter (0 to 35 Hz) was used to remove artifacts from the signal, and the bilateral mastoid leads (TP9 and TP10) were chosen for electrode re-referencing of the data. Independent component analysis (ICA) was applied to the data, and the Adjust plug-in was used to reduce artifacts caused by blinking, muscle tension, and other factors. According to the mark, the data 300 ms before P stimulation and 1000 ms after stimulation were extracted, comprising an epoch. The data 300 ms before the P stimulus was employed as the baseline for baseline correction per epoch to investigate the influence of the P stimulus on individuals.

ERP was obtained for both types of subjects through stacked averaging across every 5 epochs. Fig. 3 shows the ERP of a randomly selected liar and a truthful individual on three electrodes. It can be observed that the signal-to-noise ratio has increased and the ERP waveform of the lying subject has become more prominent. This suggested that simple time-domain averaging might be beneficial for subsequent feature extraction and classification. Fig. 2(b) depicts the signal pre-processing, where all experimental data were judged valid in this study, and the raw EEG data were preprocessed to obtain 400 30 \times 650 datasets for the deception and innocent groups, respectively.

D. WDFBN Construction

1) *Normalized Phase Transfer Entropy*: Before constructing a brain network, the network's nodes and the strength of the

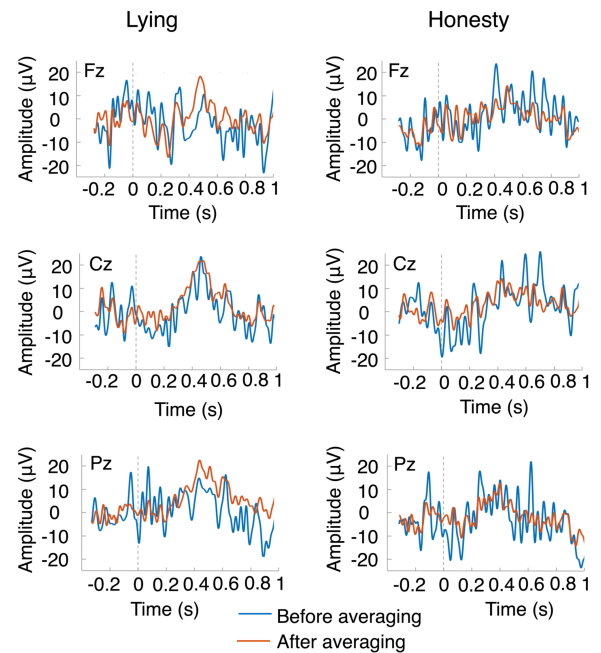


Fig. 3. Comparison of the ERP waveforms of the two types of subjects. The blue curve and the orange curve represent the signal before and after stacking averaging, respectively.

connecting edges must be determined. This study considered the EEG electrode channels as network nodes, and PTE was used to estimate the strength of the information flow between different nodes as the strength of the connecting edge. PTE and transfer entropy (TE) [40] algorithms share the same principle of studying the causal relationship of information transfer between the variables. In the information-theoretic criterion, the information transfer from both the source and the target signal's past results in a more significant reduction of target

signal uncertainty than the reduction of target signal uncertainty by the target signal's past information. This can be interpreted as a causal relationship between the source and target signals. Measuring the causal relationship between the variables of a nonlinear system is widely used in the nonlinear analysis of neural signals. If the uncertainty of the target signal $Y(t)$ at delay δ is represented by Shannon Entropy, then the TE from the source signal $X(t)$ to the target signal $Y(t)$ can be expressed as:

$$\begin{aligned} TE_{xy} &= H(Y_{t+\delta}, Y_t) + H(X_t, Y_t) - H(Y_t) - H(Y_{t+\delta}, Y_t, X_t) \\ &= \sum p(Y_{t+\delta}, Y_t, X_t) \log \left(\frac{p(Y_{t+\delta} | Y_t, X_t)}{p(Y_{t+\delta} | Y_t)} \right) \end{aligned} \quad (1)$$

where Shannon Entropy is defined as: $H(Y_{t+\delta}) = -\sum p(Y_{t+\delta}) \log p(Y_{t+\delta})$, this requires estimating the probability of all data with a discrete time step of t . However, directly estimating the probabilities of the observed data is time-consuming. Thus, Staniek and Lehnertz [41] estimated TE by turning the observed time series into a symbolic series to solve this challenge. Similarly, the signal's amplitude and instantaneous phase can be utilized to define the time series, and the transfer entropy can then be approximated from the instantaneous phase time series, resulting in the PTE algorithm. PTE is robust and offers high computational efficiency, suitable for estimating the directed connections in large-scale brain networks. For a source signal $X(t)$ the analytical signal to obtain its instantaneous phase $\theta_x(t)$, is defined as:

$$S(t) = X(t) + i \tilde{X}(t) = A(t) \exp(i \theta_x(t)) \quad (2)$$

where $A(t)$ is the instantaneous amplitude of the signal $X(t)$ and the function $\tilde{X}(t)$ is the Hilbert transform of $X(t)$, defined as:

$$\tilde{X}(t) = \frac{1}{\pi} \int_{-\infty}^{+\infty} \frac{X(\tau)}{t - \tau} d\tau \quad (3)$$

Similarly, (2) and (3) are used to calculate the instantaneous phase $\theta_y(t)$ for the target signal $Y(t)$. In this study, the Hilbert transform was applied to the signal to obtain the instantaneous phase using MATLAB's algorithm. After obtaining the signal's instantaneous, PTE of the signal $X(t)$ to $Y(t)$ is defined as:

$$\begin{aligned} PTE_{xy} &= H(\theta_y(t + \delta), \theta_y(t)) + H(\theta_y(t), \theta_x(t)) \\ &\quad - H(\theta_y(t)) - H(\theta_y(t + \delta), \theta_y(t), \theta_x(t)) \\ &= \sum p(\theta_y(t + \delta), \theta_y(t), \theta_x(t)) \log \left(\frac{p(\theta_y(t + \delta) | \theta_y(t), \theta_x(t))}{p(\theta_y(t + \delta) | \theta_y(t))} \right) \end{aligned} \quad (4)$$

where $\theta_y(t + \delta)$ is the instantaneous phase time series of the target signal $Y(t)$ at delay δ . The probability of the data is calculated through a histogram that splits the interval spanned by the data values into equal sub-intervals, places the data values in each sub-interval, counts their frequencies, and calculates the probability of each sub-interval. The histogram's width was set to: $\text{binsize} = 3.49 * \text{mean}(\text{std}(\theta)) * N_s^{-1/3}$ and the prediction delay δ was set to: $\delta = (N_s \times N_{ch}) / N_{\pm}$, where N_s and N_{ch} are the number of samples and channels respectively, and

N_{\pm} is the number of phase reversals. θ is the instantaneous phase matrix of the signal. To eliminate inaccuracy and better represent the difference in information intensity between the two types of participants' zones of interest, the PTE was normalized as:

$$dPTE_{xy} = \frac{PTE_{xy}}{PTE_{xy} + PTE_{yx}} \quad (5)$$

dPTE [37] has a maximum value of 1 and a minimum value of 0. When the dPTE ranges within (0.5, 1], it signifies that information flows from signal $X(t)$ to signal $Y(t)$, with signal $X(t)$ being the cause and signal $Y(t)$ the effect. When the range of dPTE is [0, 0.5), it means that the information flow is from signal $Y(t)$ to signal $X(t)$, with the former being the cause and the latter the effect. When the value of dPTE is 0.5, the information flow between the two leads is in equilibrium.

2) Feature Preprocessing: To positively identify lying EEG signals, the signal processing should also include feature extraction, feature selection, smoothing, and dimensionality reduction of the features. The instantaneous phase of a time series can be determined more precisely if a signal band is narrow [42]. The frequency range of the preprocessed EEG data in this investigation was 0–35 Hz, which encompassed the delta band (0–3 Hz), theta band (4–7 Hz), alpha band (8–13 Hz), and beta band (14–30 Hz), as illustrated in the second row of Fig. 2(b). The EEG signal was band-pass filtered to obtain the four sub-band signals. The Hilbert transform [43] was used to represent the EEG signal in the complex plane to extract the instantaneous phase of each frequency sub-band, and the phase angle was then calculated from the original signal and the transformed analytic signal. After calculating the instantaneous phase of the time series, a MATLAB code was written to compute the PTE between the phases of each pair of electrode channels using the histogram and the delay parameters δ . Finally, from (5), the acquired PTE was normalized to obtain the dPTE. The above approach extracted features from the honesty and lying groups' EEG signals and constructed 400 30×30 effective connectivity matrices, respectively.

After calculating each channel and band for all samples, 870 channel combinations in each sub-band required analysis, and most of these features were not statistically different, so we had to select the features, as depicted in the third row of Fig. 2(b). The entropy values of the channel combination features in the matrix were compared between the groups to identify meaningful, connected features with statistical differences. A non-parametric permutation test ($Np = 10000$) [44] was performed on the dPTE values for all channel combinations to find the ones that were statistically substantially different, to reduce the effect of computational bias. After the permutation test, only the significant values were considered, while the inconsequential values were set to zero.

The feature sets with significant differences contain all vital information and may have redundant information, degrading the classifier's performance [45]. In practical applications, feature dimensionality reduction improves the convergence speed and the classifiers' stability [46]. Therefore, to avoid feature redundancy and reduce the number of inputs to the classification model features and accelerate network convergence, this study reduces

TABLE I
HYPERPARAMETERS FOR THE OPTIMAL MODEL

parameter	Lie prediction model based on CatBoost
Max number of tree	500
Depth of the tree	6
Learning Rate	0.1
Loss function	MultiClass

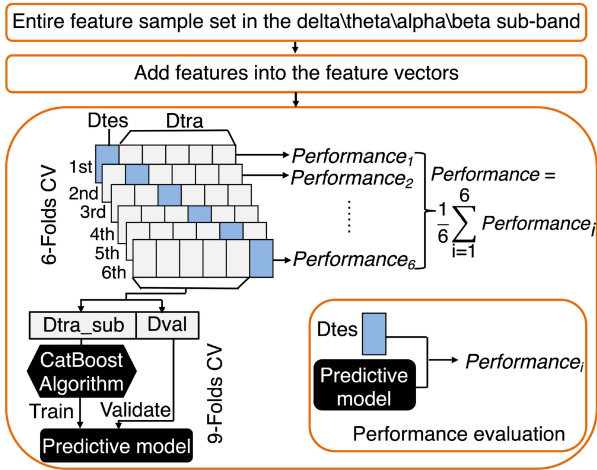


Fig. 4. Flow chart of classification. Performance indicates the effect of the lying predictive model. CV: cross-validation.

the feature dimensionality based on L1-regularized logistic regression [47] and searches for the subset of features that are most relevant to predicting whether a subject is lying or not. This method's core principle is to train all features using a logistic regression algorithm, model them with an L1 parity as the penalty term, obtain the weight coefficients for each feature, and select the features based on the coefficients from the largest to the smallest. Since the smaller the penalty term coefficient C , the fewer features are selected, this article set C to 0.1, considering that a large number of features increases the difficulty of the brain network analysis.

3) *Building the Lying Predict Model*: A proficient classifier determines the difference between individuals who lie and those who are truthful. This work applied the CatBoost [48] machine learning classification method for deception detection. In addition to addressing the gradient and prediction bias problems. The algorithm has the advantages of resilience (cutting the need for significant hyperparameter tuning) and great performance. Table I reports the ideal hyperparameters of the prediction model for CatBoost based classification prediction of deception and innocence on Python 3.6. During classification, the features selected after the dimensionality reduction process were added to the classifier. Fig. 4 reveals that a nested cross-validation (CV) [49] scheme was used to estimate the prediction model's weights and hyperparameters. A 6-Folds CV strategy was applied to each feature subset, with the samples randomly divided into training and test sets, where **Dtra** and **Dtes** adopted a 5:1 ratio. Then, 9-Folds CV was applied on the training set, with

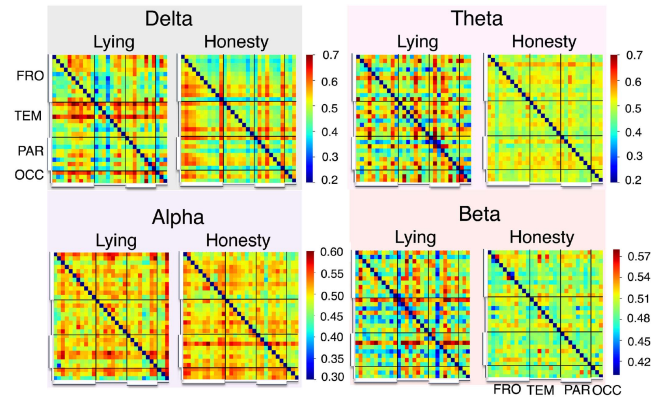


Fig. 5. Comparison of group average dPTE effectivity connection matrix for all bands. Each electrode channel is represented by a row and column in the matrix. The link weight from the horizontal electrode channel to the vertical electrode channel is measured by each node element, which is color coded. Solid vertical lines separate the brain areas corresponding to the electrode channels in the matrix, which are the frontal (FRO), temporal (TEM), parietal (PAR), and occipital (OCC) lobes, from left to right.

Dtra randomly partitioning into training subset **Dtra_sub** and validation set **Dval** in an 8:1 ratio. In the inner loop of the nested cross-validation, the hyperparameters were continuously updated to construct six classifiers, and the classifier's output was the average value of **Dtes** predicted by the classifier. To test CatBoost's ability to predict lying and honesty, the model parameters of the LR [50] and SVM [51] classifiers were adjusted to optimize the model, and their performance were compared using the same training set as CatBoost.

III. RESULTS

A. dPTE as Metrics of Identifying Lies

1) *dPTE Effectivity Connection Matrix*: The group average connection matrix of the four bands was generated by extracting the features of each band using the dPTE. The adjacency matrix of all the samples was illustrated in Fig. 5. The darker the grid color in the diagram, the stronger the information interaction between the channels. In the delta band, we found stronger information interaction between the temporal lobe and other brain regions in the lying group than in the honesty group. The difference in the occipital lobe between the two groups of subjects in the Alpha band was more evident. Considering the theta and beta bands, the dPTE values of the honesty group connectivity matrix converged to 0.5, indicating that the information flow between the channels was in balance, implying that the subjects' brains responded honestly in these two bands were not significantly activated.

2) *Statistical Analysis of Classification Results*: This study used feature preprocessing to find the statistically significant dPTE values between the frequency groups. The non-parametric replacement was tried on all features in the four frequency bands of the two subject groups, and only the statistically different features were chosen. Furthermore, feature dimensionality reduction was performed on the selected features based on an L1-regularized logistic regression. After this operation, the

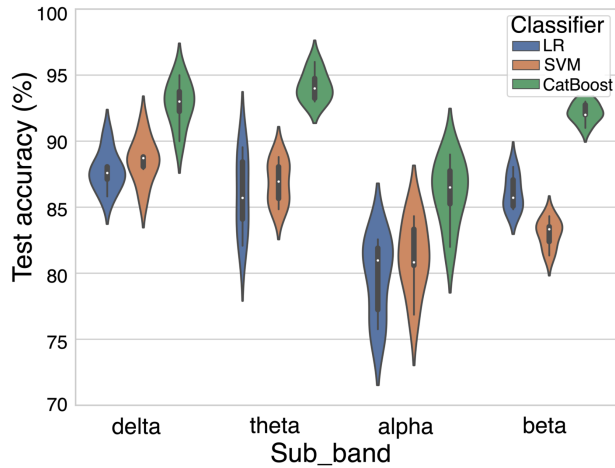


Fig. 6. Comparison chart of classification accuracy of linear regression (LR), support vector machine (SVM) and CatBoost. The white dots on the violin chart indicated the median. The black box plot indicated the range of test accuracy.

number of feature dimensions remaining in the delta band was 7, the theta band was 3, the alpha band was 2, and the beta band was 4.

The selected features were added to the feature set as classification features for the LR, SVM, and CatBoost classifiers. The output values of all classifiers were used to assess the model's prediction performance. Fig. 6 illustrates the test accuracy of the three classifiers in the four frequency bands, highlighting that the accuracy of the two comparison models, LR and SVM, was concentrated between 85% and 90% in the delta and theta bands and between 80% and 85% in the alpha and beta bands. Compared to the comparison models, the accuracy of the CatBoost model was concentrated between 90% and 95% in the delta, theta, and beta bands and between 85% and 90% in the alpha. Additionally, the black box range demonstrates that the accuracy of CatBoost fluctuates is inferior to the other models, implying that the classifier is more efficient and robust. Therefore, the CatBoost was chosen as the feature classifier for this article. Indeed, the average classification accuracy was 92.83% for the delta band, 94.17% for the theta band, 85.93% for the alpha band, and 92.25% for the beta band.

B. WDFBN Analysis

According to the classification statistics mentioned above, the features selected for this study can be distinguished between honest and lying subjects. The mean dPTE group difference of the classification features was illustrated in Fig. 7, revealing that the difference in dPTE exceeds 0.1 for all bands except for the beta band.

To more intuitively highlight the brain's information flow patterns in different frequency bands during the deception state and to explore the relevant information of the cerebral cortex functional areas, mapping the scalp EEG data to the cerebral cortex is required. Currently, there are two commonly used mapping methods in research: source localization method [52], [53] and automatic mapping EEG signal to cortex method [54],

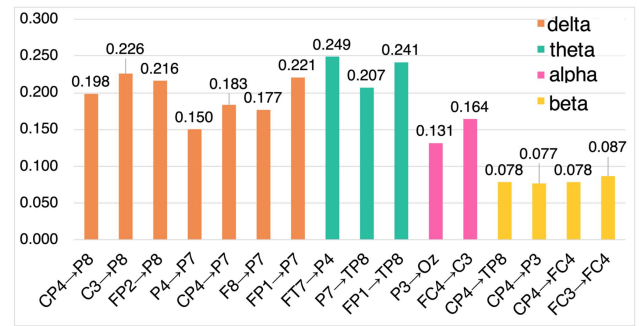


Fig. 7. Difference of group mean of the dPTE in each frequency band. The horizontal coordinate indicated the name of the lead pair and the vertical coordinate indicated the dPTE value.

[55]. The source localization method determines the source position of the signal by analyzing the features in the EEG data, but the calculation complexity is high and the mapping results are not very intuitive. In comparison, the method of automatically mapping the EEG signal to the cortex utilizes the correspondence between the electrode position and the three-dimensional structure of the brain cortex to map the EEG data to the brain cortex, which is simple and straightforward, and the mapping results are intuitive. Therefore, this study chose the method of automatic mapping to map the EEG data onto the Brodmann area of cerebral cortex (the corresponding band and brain region names are shown in Table II) and plotted the information flow maps of the WDFBN for the four bands using BrainNet Viewer [56] (Fig. 8). As illustrated in Fig. 8, the information flow is primarily transferred from the inferior parietal and superior frontal gyrus to the inferior temporal gyrus in the delta band. Indeed, the theta band was more complicated and involved more brain regions, but the primary pattern of information flows originated from the superior temporal gyrus to the inferior parietal gyrus and from the prefrontal cortex to the middle temporal. In the alpha band, the information flows mainly from the middle frontal gyrus to the postcentral gyrus and from the precuneus to the cuneus. The information flows mainly from the inferior parietal gyrus to other brain regions in the beta band.

IV. DISCUSSION

This study aims to investigate the patterns of information interaction in the brain during deception. To our knowledge, WDFBN was exploited for the first time in lie detection using the dPTE algorithm. dPTE is a phase-based information flow method used to estimate the directional connection between the signals of each lead. It is a valuable tool for studying the brain's functional network in the process of lie cognition. This research revealed the functional connections between active brain regions and the information flow patterns between distinct brain regions, allowing researchers to investigate cognitive differences between deception and truth in specific frequency sub-bands, and the mechanics of neural activity in the brain during deception conditions.

The neural oscillations driving lying and integrity were evaluated based on the effective network connections to recognize

TABLE II
EACH FREQUENCY BAND ELECTRODE AND ITS CORRESPONDING PROJECTION CORTICAL AREA

Channel	Brodmann area	Abbreviations	Coordinates	Sub-band
Frontal cortex				
FP1	L Superior Frontal Gyrus	SFG (10L)	-21.2, 58.9, 12.1	delta, theta
FP2	R Superior Frontal Gyrus	SFG (10R)	24.3, 58.3, 12.5	delta
FC3	L Middle Frontal Gyrus	MFG (6L)	-45.5, 2.4, 51.3	beta
FC4	R Middle Frontal Gyrus	MFG (6R)	47.5, 4.6, 49.7	alpha, beta
F8	R Inferior Frontal Gyrus	IFG (45R)	51.2, 28.4, 3.1	delta
Temporal cortex				
P7	L Inferior Temporal Gyrus	ITG (37L)	-48.9, -64.8, 0	delta, theta
P8	R Inferior Temporal Gyrus	ITG (19R)	48.4, -64.4, 0.1	delta
FT7	L Superior Temporal Gyrus	STG (22L)	-59.2, 3.4, -2.1	theta
TP8	R Middle Temporal Gyrus	MTG (21R)	60.6, -45.4, -3.7	theta, beta
Parietal cortex				
C3	L Postcentral Gyrus	PoCG (123L)	-49.1, -20.7, 53.2	delta, alpha
CP4	R Inferior Parietal Gyrus	IPG (40R)	49.5, -45.5, 48.7	delta, beta
P3	L Precuneus	PCUN (18L)	-41.4, -67.8, 42.4	alpha, beta
P4	R Inferior Parietal Gyrus	IPG (7R)	44.2, -65.8, 40.7	delta, theta
Occipital cortex				
Oz	M Cuneus	Cuneus (18M)	3.0, -94.1, 8.7	alpha

R, right; L, left; M, middle.

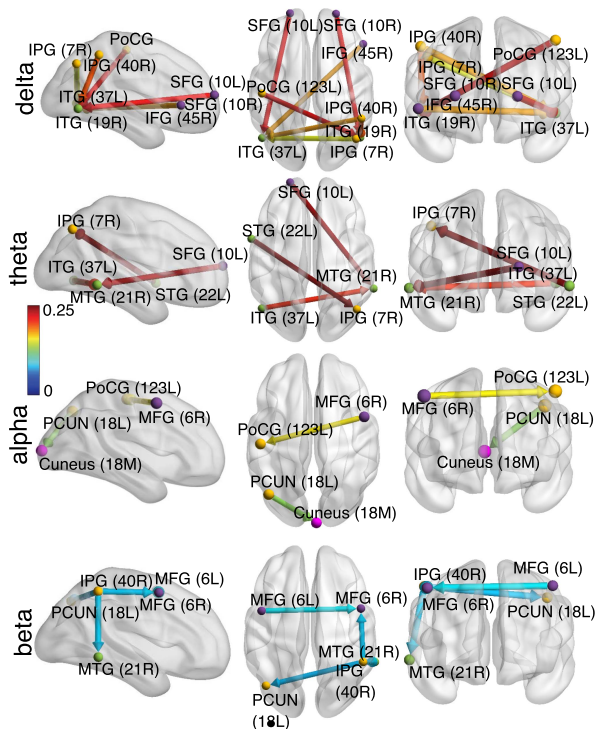


Fig. 8. WDFBN for each frequency band. Color of the nodal connection line in the brain area corresponds to the group average dPTE difference value for each frequency band, indicating the strength of information flow. Direction of the arrow denotes the preferred information flow direction. Nodes indicate the selected electrode channel, and the node color indicates the brain area. Purple, green, yellow and pink denote the frontal, temporal, parietal and occipital lobes.

functional connectivity patterns and information transfer between brain areas during deception. The experimental results provide direction for future research on the information flow in the human brain during lie detection. Here, we analyzed different frequency bands, and found that the dPTE in the brain was

significantly higher in the lower frequency bands (delta and theta) than in the higher frequency bands (alpha and beta) (Fig. 8), particularly in the information flow pattern of the prefrontal-temporal pathway. Previous research has also observed an increase in this pathway activity during lying [17], [21]. The prefrontal lobe was activated in all frequency sub-bands, and the information interaction between the frontal lobe and the rest of the cortex better reflected the difference between lying and honesty, indicating that the frontal lobe performed an essential role in the neural circuitry of deception. The linkages connected with the frontal-parietal network and the temporoparietal junction were the most discriminating. This demonstrated that various brain parts were active throughout lying, and the connections between these areas were enhanced, while the information interchange increased more frequently. Previous fMRI research has confirmed that lying increases activity in the frontal, temporal and parietal cortices compared to speaking the truth [24], [57], and this study confirm these main results in those research.

A. Delta

Currently, there are two main origins of delta identified: one is thalamus, which is more researched and linked to sleep [58], and the other is cerebral cortex, which may be linked to higher cognitive processes in humans. P300 [12], [23] is one of the most well-known ERP components, with delta low-frequency oscillations contributing the most to the P300 [59]. P300 has been proven to reflect higher cognitive human skills, such as perception, attention, comprehension, and judgment [60], [61]. As a result, delta oscillations play an essential role in human attention. When lying, a person's brain will allocate attention to suppress the exposure of false information [62]. If the liar feels uneasy or nervous about the lie they are telling, attention distribution becomes more focused, resulting in the liar exhibiting certain specific neural physiological features, such as the delta

oscillations energy increases [17], [31]. Our results also showed this phenomenon, compared to the honesty group, the delta band oscillation was enhanced and the information interaction was more obvious when lying.

The act of lying often requires the liar to conceal information and manipulate the truth [63]. This requires significant cognitive effort, such as increased brain activity in regions related to attention and decision-making, to activate the brain's conflict detection system. During cognitive activities, the frontal lobes, especially the prefrontal cortex and dorsolateral prefrontal cortex (DLPFC), can be flexibly linked to other brain networks and involved in a wide range of cognitive processes, making them an essential part of deceptive cognitive tasks [64], [65]. Recent neuroimaging studies have revealed that the DLPFC is involved in attention-related cognitive processes and monitors salient motivational stimuli, particularly in decision-making responses [66], [67]. The findings of another study suggested that there may have been a relation between the increase in delta amplitude in the odd paradigm and decision-making responses [68]. Consistent with these prior studies, our results suggested that an increase in delta band dPTE was particularly noticeable, especially the connection between the frontal and temporal regions. The angular gyrus was assumed to have a role in attentional mechanisms, and the temporal area was considered vital for long-term memory. Some studies have already proven that the prefrontal-temporal pathway is primarily responsible for functions such as memory, attention, and decision-making [69], [70]. As a result, the information flow from the SFG (10L), SFG (10R), and IFG (45R) to the ITG might indicate that the deception group inadvertently paid attention and remembered the crime procedure or specifications whenever they came across something related to the stolen object or the crime scene. Furthermore, activation of the frontal and temporal lobe areas of the brain enhances the exchange of information between these areas, which may be related to the need to allocate more executive control and attentional resources to monitoring and resolving conflicting information. This helps ensure that the brain processes lying information consistently and meaningfully.

In the delta band WDFBN, the interaction of information between the parietal and temporal lobe was also relatively strong during deception. Suzuki et al. [71] have shown that the posterior parietal cortex is engaged in memory updating. The P300 component of endogenous ERP produced by the deception test was most visible in the parietal lobule [11]. Processing the social environment and psychoanalyzing the intentions and mental states of others involved temporal and parietal areas [72], [73]. Combined with the results of previous studies, an information flow pattern from the IPG (7R) and IPG (40R) to ITG (37L), PoCG (123L) to ITG (37R) might demonstrate that choosing to say something false and making decisions involves a mental differentiation between truth and untruth. It is critical to make a concerted effort to convince people to believe falsehoods, which is risky. As a result, the subject must bear a greater psychological burden and display meaningful brain activity in their temporoparietal control network. This adds to the growing evidence that the temporoparietal area was activated and revealed the this area's information transmission pattern

during deception. It also confirms that the delta oscillation is linked to higher cognitive activities like attention and judgment. The results of the analysis of the delta band showed that, at least two distinct interactive critical loop play a role in lying: the frontotemporal circuitry involved in conflict-monitoring and the temporoparietal circuitry involved in self-related mental simulations.

B. Theta

The study found that the connectivity between ITG (19R) and MTG (21R) in the theta sub-band was strengthened in the deception condition. Memory processes, the temporal lobe and theta oscillations have now been connected in numerous studies [74], [75], [76], revealing that working memory activities cause theta oscillations [77]. As a result, this effective connectivity in the temporal lobe may indicate that familiar P stimuli elicited people's visual attention, and then subjects recalled and processed the memory information stored in the brain. Additionally, it could be found a pattern of information flow from SFG (10L) to MTG (21R) and STG (22L) to IPG (7R). This suggested that the brain adjusts the activity of the frontal, temporal and parietal to control emotional expression, evaluate risks and conceal true information when subject chose to lie. Since the network was built based on dPTE, it could be considered that the links were indicators of the flow of information between nodes. Therefore, the findings of theta band might be considered as a sign of more information transfer from frontal to temporal and temporal to parietal in liars. Another explanation of this result was that, in the process of lying. First, the prefrontal lobe collaborated with the medial temporal lobe in making decisions and in assessing risks for the content to be lied about. Second, the temporal lobe collaborates with the inferior parietal gyrus in suppressing the truth and in updating memory, thus forming a prefrontal—medial temporal—inferior parietal gyrus neural circuit, which was closely related to the processing of lie information.

C. Alpha

Alpha rhythms might be classified into two types based on the cortical areas where they occur: alpha oscillations in sensory-motor cortical areas [78] and alpha rhythms in the visual cortex or occipital lobe [79]. Previous research has indicated that increasing alpha activity is beneficial for suppressing distracting input [80], [81]. Langleben et al. used the GKT paradigm and found increased activity at the intersection of the prefrontal and anterior parietal cortices when subjects exhibited deceptive responses by pressing a button. They suggested that this may be related to increased demands on motor control [82]. Zhou et al. have found that alpha oscillation phase in the parietal, frontal, and occipital regions of the brain prior to stimulus presentation can modulate perceptual accuracy in visual tasks [83]. In this study, an increased information flow in the alpha band was observed between MFG (6R) and PoCG (123L), which might indicate that participants will predict an impending stimulus, and when the observed object matches the predicted object, the communication between the midfrontal gyrus and postcentral gyrus of the brain became more efficient, which in turn contributed to

supporting cognitive control processes of visual attention and response inhibition.

Early studies [84], [85] found that alpha band activity is strongly modulated during working memory tasks, with an increase in alpha being a result of functional inhibition. Palva et al. [86] further observed that increasing task load leads to enhanced phase synchrony, with the most prominent effects observed in alpha band oscillations. Additionally, considering that alpha oscillation is the dominant EEG activity in the occipital region, an increased connectivity was observed between PCUN (18L) and Cuneus (18M) during the processing of P stimuli, indicating the activation of the occipital cortex. It can be speculated that enhanced alpha band oscillations observed during high cognitive demand tasks may contribute to increased connectivity between brain regions, which may have allowed the occipital cortex to jointly inhibit conflict memory with the precuneus to achieve deception.

D. Beta

In a visual task for predicting trust, Wang et al. found that the trust condition led to an increase in beta-band activity in the frontocentral cortex and suggested that this may be related to cognitive inhibition [87]. Huster et al. investigated cognitive control processes using a stop signal and go/no-go paradigm, and found increased beta-band activity in the inferior frontal gyrus and primary motor cortex during the stop trials, likely reflecting the continuation of the previous motor response when the stop signal appears and no response is made [88]. Additionally, Andreas et al. suggested that stronger beta oscillations in the primary motor cortex were associated with maintaining activity related to current sensorimotor or cognitive states [89]. Observing the beta WDFBN, the dPTE connection involving the premotor and supplementary motor cortex was: MFG (6L) to MFG (6R). Therefore, we could infer that when the criminal signal appeared, the response made by the lying group needed to be consistent with the other stimulus signals, so it was necessary to inhibit the previous memory information and maintain the previous sensory motor state. This process was achieved by enhancing the information interaction between the left and right middle frontal gyrus in the beta frequency band.

The other three connections in the WDFBN involved the middle frontal gyrus, inferior parietal gyrus, middle temporal gyrus, and precuneus. Husain et al. speculated that many classic parietal functions are provided by different regions within the frontoparietal network, and that visual selective attention may also be impaired when this network is damaged [90]. Corbetta et al. suggested that when salient stimuli appear, temporoparietal junction will reallocate attention in a stimulus-driven manner [91]. Treserras et al. explored how the brain transitions from rest to movement and found that the precuneus is a key area in preparing for movement. Additionally, functionally, the precuneus works in conjunction with the medial superior parietal cortex to initiate motor encoding [92]. Therefore, compared with the honesty group, the information flow from IPG (40R) to MFG (6R), MTG (21R), and PCUN (18L) were increased in the lying group, which might indicate that when the P stimulus (salient

stimulus) appears, the brain directs attention to the salient event through the frontoparietal and the temporoparietal network, followed by the cooperation between the inferior parietal lobule and the precuneus to initiate the button response. In general, the WDFBN in the beta band showed that multiple functional networks were involved in completing the lying behavior, especially the selective attention network and the motor control network.

V. CONCLUSION, LIMITATIONS, AND FUTURE WORK

This work proposed an intelligent lie detection system based on EEG signals. This study intended to see whether there were any variations between the WDFBN of dishonest and honest persons. First, the dPTE values between the lead pairs were calculated, and the dimensionality of feature values was reduced by logistic regression with L1 regularization terms. Following that, nested cross-validation was used to train and test classifiers, including SVM, LR, and CatBoost, and satisfactory classification results were obtained. In comparison to SVM and LR, CatBoost achieved higher classification accuracy. This study revealed that using a machine learning classifier with phase transfer entropy feature extraction methods to analyze EEG signals was appealing for detecting honesty and lying. The findings in the WDFBN revealed strong information interactions among the frontotemporal network in the delta and theta bands, and the frontoparietal network in the alpha and beta band, indicating that these two networks play an important role in deception processing. The analysis of various frequency bands found that the increased information exchange between the delta, alpha, and beta band brain regions may be related to executive control of attention, visual attention, and selective attention, respectively.

Exploring cognitive activity in the brain during deception can enhance our understanding of the phenomenon of lying in cognitive psychology and shed light on the information processing mechanisms of the human brain. This study aimed to create a WDFBN for the EEG data elicited by P-stimulation in the deception state and investigate the causal links between brain regions based on the network's information flow patterns. Our findings largely corroborated the findings of prior lying studies and provided new insights into brain oscillations during deception.

Although our findings provide insight into the information interaction pattern of lying neural oscillations, our research has some limitations. First, this study only conducted cross-group analysis and confirmed differences between the two groups of liars and truth tellers, but it is unsure whether these results are consistent in cross-time studies. Therefore, future research goal is to combine cross-group studies with cross-time studies to validate the robustness of our conclusions. Second, the computation of the brain functional network in this study is based on the entire time before and after the stimulus, therefore the frequency band analysis cannot locate the event-related processing in different time stages of the brain. Future work could adopt clustering or hidden Markov methods to construct an event-related dynamic brain functional network and better explore the event-specific temporal variations in brain processing. Third, although EEG

can capture instantaneous changes in brain electrical activity, its spatial resolution is poorer compared to fNIRS and fMRI. Therefore, future studies can combine EEG and fNIRS or EEG and fMRI to more study the relationship between brain activity and lying behavior accurately. Finally, this study only intuitively mapped the scalp EEG signals to the cortex, and future work should use source analysis to study the directional connections of the functional network in the brain cortex and conduct more in-depth research on the mechanisms of lying.

Conflict of Interest: The authors have declared that no competing interests exist.

REFERENCES

- [1] A. Turri and J. Turri, "The truth about lying," *Cognition*, vol. 138, pp. 161–168, May 2015.
- [2] J. Gao et al., "Brain fingerprinting and lie detection: A study of dynamic functional connectivity patterns of deception using EEG phase synchrony analysis," *IEEE J. Biomed. Health Inform.*, vol. 26, no. 2, pp. 600–613, Feb. 2022.
- [3] A. Vrij, R. P. Fisher, and H. Blank, "A cognitive approach to lie detection: A meta-analysis," *Legal Criminological Psychol.*, vol. 22, no. 1, pp. 1–21, Jan. 2017.
- [4] J. Gao et al., "Denoised P300 and machine learning-based concealed information test method," *Comput. Methods Prog. Biomed.*, vol. 104, no. 3, pp. 410–417, Dec. 2011.
- [5] C. R. Honts, D. C. Raskin, and J. C. Kircher, Eds., *Credibility Assessment: Scientific Research and Applications*. Amsterdam, The Netherlands: Elsevier, 2013.
- [6] A. Vrij et al., "Detecting deceit via analysis of verbal and non-verbal behavior," *J. Nonverbal Behav.*, vol. 24, no. 4, pp. 239–263, Dec. 2000.
- [7] J. Synnott, D. Dietzel, and M. Ioannou, "A review of the polygraph: History, methodology and current status," *Crime Psychol. Rev.*, vol. 1, no. 1, pp. 59–83, Jan. 2015.
- [8] A. C. Jenkins, L. Zhu, and M. Hsu, "Cognitive neuroscience of honesty and deception: A signaling framework," *Curr. Opin. Behav. Sci.*, vol. 11, pp. 130–137, Oct. 2016.
- [9] N. Abe, "How the brain shapes deception: An integrated review of the literature," *Neuroscientist*, vol. 17, no. 5, pp. 560–574, Mar. 2011.
- [10] K. Suchotzki et al., "The cognitive mechanisms underlying deception: An event-related potential study," *Int. J. Psychophysiol.*, vol. 95, no. 3, pp. 395–405, 2015.
- [11] T. W. Picton, "The P300 wave of the human event-related potential," *J. Clin. Neurophysiol.*, vol. 9, no. 4, pp. 456–479, Oct. 1992.
- [12] T. R. Cutmore et al., "An object cue is more effective than a word in ERP-based detection of deception," *Int. J. Psychophysiol.*, vol. 71, no. 3, pp. 185–192, Mar. 2009.
- [13] E. H. Meijer et al., "The P300 is sensitive to concealed face recognition," *Int. J. Psychophysiol.*, vol. 66, no. 3, pp. 231–237, Dec. 2007.
- [14] J. B. Meixner and J. P. Rosenfeld, "Countermeasure mechanisms in a P300-based concealed information test," *Psychophysiology*, vol. 47, no. 1, pp. 57–65, Dec. 2010.
- [15] E. Labkovsky and J. P. Rosenfeld, "The P300-based, complex trial protocol for concealed information detection resists any number of sequential countermeasures against up to five irrelevant stimuli," *Appl. Psychophysiol. Biofeedback*, vol. 37, pp. 1–10, Mar. 2012.
- [16] A. Bablani et al., "An efficient concealed information test: EEG feature extraction and ensemble classification for lie identification," *Mach. Vis. Appl.*, vol. 30, pp. 813–832, Jul. 2019.
- [17] J. Gao et al., "Effective connectivity in cortical networks during deception: A lie detection study based on EEG," *IEEE J. Biomed. Health Inform.*, vol. 26, no. 8, pp. 3755–3766, Aug. 2022.
- [18] D. Wu et al., "Neural correlates of evaluations of lying and truth-telling in different social contexts," *Brain Res.*, vol. 1389, pp. 115–124, May 2011.
- [19] L. Sai et al., "Neural mechanisms of deliberate dishonesty: Dissociating deliberation from other control processes during dishonest behaviors," *Proc. Nat. Acad. Sci.*, vol. 118, no. 43, Oct. 2021, Art. no. e2109208118.
- [20] H. Gibbons et al., "Detection of deception: Event-related potential markers of attention and cognitive control during intentional false responses," *Psychophysiology*, vol. 55, no. 6, Jun. 2018, Art. no. e13047.
- [21] W. Chang et al., "Comparison of different functional connectives based on EEG during concealed information test," *Biomed. Signal Process. Control*, vol. 49, pp. 149–159, Mar. 2019.
- [22] X. P. Ding et al., "Neural correlates of spontaneous deception: A functional near-infrared spectroscopy (fNIRS) study," *Neuropsychologia*, vol. 51, no. 4, pp. 704–712, Mar. 2013.
- [23] L. Sai et al., "Telling a truth to deceive: Examining executive control and reward-related processes underlying interpersonal deception," *Brain Cogn.*, vol. 125, pp. 149–156, Aug. 2018.
- [24] J. Yu et al., "Can fMRI discriminate between deception and false memory? A meta-analytic comparison between deception and false memory studies," *Neurosci. Biobehavioral Rev.*, vol. 104, pp. 43–55, Sep. 2019.
- [25] J. J. Walczyk and C. Fargerson, "A cognitive framework for understanding development of the ability to deceive," *New Ideas Psychol.*, vol. 54, pp. 82–92, Aug. 2019.
- [26] J. Wyman, H. Cassidy, and V. Talwar, "Utilizing the activation-decision-construction-action theory to predict children's hypothetical decisions to deceive," *Acta Psychol.*, vol. 218, Jul. 2021, Art. no. 103339.
- [27] N. Hollenstein et al., "Decoding EEG brain activity for multi-modal natural language processing," *Front. Hum. Neurosci.*, vol. 15, Jul. 2021, Art. no. 378.
- [28] P. Li et al., "EEG based emotion recognition by combining functional connectivity network and local activations," *IEEE Trans. Biomed. Eng.*, vol. 66, no. 10, pp. 2869–2881, Oct. 2019.
- [29] K. W. Ha and J. W. Jeong, "Motor imagery EEG classification using capsule networks," *Sensors*, vol. 19, no. 13, Jun. 2019, Art. no. 2854.
- [30] N. Lisofsky et al., "Investigating socio-cognitive processes in deception: A quantitative meta-analysis of neuroimaging studies," *Neuropsychologia*, vol. 61, pp. 113–122, Aug. 2014.
- [31] P. Liu et al., "Functional connectivity pattern analysis underlying neural oscillation synchronization during deception," *Neural Plast.*, vol. 2019, Feb. 2019, Art. no. 2684821.
- [32] N. Ahmadi et al., "EEG-based classification of epilepsy and PNES: EEG microstate and functional brain network features," *Brain Inf.*, vol. 7, pp. 1–22, Dec. 2020.
- [33] X. Shao et al., "Analysis of functional brain network in MDD based on improved empirical mode decomposition with resting state EEG data," *IEEE Trans. Neural Syst. Rehabil. Eng.*, vol. 29, pp. 1546–1556, 2021.
- [34] Y. Wang et al., "An electroencephalography network and connectivity analysis for deception in instructed lying tasks," *PLoS One*, vol. 10, no. 2, Feb. 2015, Art. no. e0116522.
- [35] F. Hasanzadeh, M. Mohebbi, and R. Rostami, "Graph theory analysis of directed functional brain networks in major depressive disorder based on EEG signal," *J. Neural Eng.*, vol. 17, no. 2, Mar. 2020, Art. no. 026010.
- [36] M. Lobier et al., "Phase transfer entropy: A novel phase-based measure for directed connectivity in networks coupled by oscillatory interactions," *Neuroimage*, vol. 85, pp. 853–872, Jan. 2014.
- [37] A. Hillebrand et al., "Direction of information flow in large-scale resting-state networks is frequency-dependent," *Proc. Nat. Acad. Sci.*, vol. 113, no. 14, pp. 3867–3872, Mar. 2016.
- [38] M. Dauwan et al., "EEG-directed connectivity from posterior brain regions is decreased in dementia with Lewy bodies: A comparison with Alzheimer's disease and controls," *Neurobiol. Aging*, vol. 41, pp. 122–129, Feb. 2016.
- [39] A. Arasteh, M. H. Moradi, and A. Janghorbani, "A novel method based on empirical mode decomposition for P300-based detection of deception," *IEEE Trans. Inf. Forensics Security*, vol. 11, no. 11, pp. 2584–2593, Nov. 2016.
- [40] R. Vicente et al., "Transfer entropy—A model-free measure of effective connectivity for the neurosciences," *J. Comput. Neurosci.*, vol. 30, no. 1, pp. 45–67, Feb. 2011.
- [41] M. Staniek and K. Lehnertz, "Symbolic transfer entropy," *Phys. Rev. Lett.*, vol. 100, no. 15, 2008, Art. no. 158101.
- [42] M. Chavez et al., "Towards a proper estimation of phase synchronization from time series," *J. Neurosci. Methods*, vol. 154, no. 1/2, pp. 149–160, Jun. 2006.
- [43] S. L. Hahn, "Comments on 'A tabulation of Hilbert transforms for electrical engineers'," *IEEE Trans. Commun.*, vol. 44, no. 7, p. 768, Jul. 1996.
- [44] T. E. Nichols and A. P. Holmes, "Nonparametric permutation tests for functional neuroimaging: A primer with examples," *Hum. Brain Mapping*, vol. 15, no. 1, pp. 1–25, Jan. 2002.
- [45] A. K. Jain, R. P. W. Duin, and J. Mao, "Statistical pattern recognition: A review," *IEEE Trans. Pattern Anal. Mach. Intell.*, vol. 22, no. 1, pp. 4–37, Jan. 2000.
- [46] A. M. Alhassan and W. M. N. Wan Zainon, "Review of feature selection, dimensionality reduction and classification for chronic disease diagnosis," *IEEE Access*, vol. 9, pp. 87310–87317, 2021.

- [47] P. Ravikumar, M. J. Wainwright, and J. D. Lafferty, "High-dimensional Ising model selection using ℓ_1 -regularized logistic regression," *Ann. Statist.*, vol. 38, no. 3, pp. 1287–1319, Jun. 2010.
- [48] L. Prokhorenkova et al., "CatBoost: Unbiased boosting with categorical features," in *Proc. Adv. Neural Inf. Process. Syst.*, 2018, pp. 6639–6649.
- [49] G. C. Cawley and N. L. C. Talbot, "On over-fitting in model selection and subsequent selection bias in performance evaluation," *J. Mach. Learn. Res.*, vol. 11, pp. 2079–2107, Jan. 2010.
- [50] P. Cohen, S. G. West, and L. S. Aiken, *Applied Multiple Regression/Correlation Analysis for the Behavioral Sciences*. London, U.K.: Psychol. Press, Apr. 2014.
- [51] C. Cortes and V. Vapnik, "Support-vector networks," *Mach. Learn.*, vol. 20, no. 3, pp. 273–297, Sep. 1995.
- [52] C. Phillips, M. D. Rugg, and K. J. Friston, "Systematic regularization of linear inverse solutions of the EEG source localization problem," *NeuroImage*, vol. 17, no. 1, pp. 287–301, Sep. 2002.
- [53] J. Song et al., "EEG source localization: Sensor density and head surface coverage," *J. Neurosci. Methods*, vol. 256, pp. 9–21, Dec. 2015.
- [54] L. Koessler et al., "Automated cortical projection of EEG sensors: Anatomical correlation via the international 10–10 system," *NeuroImage*, vol. 46, no. 1, pp. 64–72, Aug. 2009.
- [55] M. Okamoto et al., "Three-dimensional probabilistic anatomical cranio-cerebral correlation via the international 10–20 system oriented for transcranial functional brain mapping," *NeuroImage*, vol. 21, no. 1, pp. 99–111, Jan. 2004.
- [56] M. Xia et al., "BrainNet viewer: A network visualization tool for human brain connectomics," *PLoS One*, vol. 8, no. 7, Aug. 2013, Art. no. e68910.
- [57] M. Zheltyakova et al., "Neural mechanisms of deception in a social context: An fMRI replication study," *Sci. Rep.*, vol. 10, no. 1, Jul. 2020, Art. no. 10713.
- [58] L. M. Fernandez and A. Lüthi, "Sleep spindles: Mechanisms and functions," *Physiol. Rev.*, vol. 100, no. 2, pp. 805–868, Apr. 2020.
- [59] M. Schürmann et al., "Delta responses and cognitive processing: Single-trial evaluations of human visual P300," *Int. J. Psychophysiol.*, vol. 39, no. 2/3, pp. 229–239, Jun. 2001.
- [60] A. C. Ward et al., "The effect of retroactive memory interference on the P300-based complex trial protocol (CTP)," *Int. J. Psychophysiol.*, vol. 147, pp. 213–223, Jan. 2020.
- [61] V. Scheuble and A. Beauducel, "Individual differences in erps during deception: Observing vs. demonstrating behavior leading to a small social conflict," *Biol. Psychol.*, vol. 150, Feb. 2020, Art. no. 107830.
- [62] A. Pittarello et al., "The relationship between attention allocation and cheating," *Psychon. Bull. Rev.*, vol. 23, pp. 609–616, Apr. 2016.
- [63] B. Van Bockstaele et al., "Learning to lie: Effects of practice on the cognitive cost of lying," *Front. Psychol.*, vol. 3, Nov. 2012, Art. no. 526.
- [64] A. Priori et al., "Lie-specific involvement of dorsolateral prefrontal cortex in deception," *Cereb. Cortex*, vol. 18, no. 2, pp. 451–455, Feb. 2008.
- [65] F. Marneli et al., "Dorsolateral prefrontal cortex specifically processes general—but not personal—knowledge deception: Multiple brain networks for lying," *Behav. Brain Res.*, vol. 211, no. 2, pp. 164–168, Jun. 2010.
- [66] J. T. Buhle et al., "Cognitive reappraisal of emotion: A meta-analysis of human neuroimaging studies," *Cereb. Cortex*, vol. 24, no. 11, pp. 2981–2990, Nov. 2014.
- [67] E. S. Allard and E. A. Kensinger, "Age-related differences in neural recruitment during the use of cognitive reappraisal and selective attention as emotion regulation strategies," *Front. Psychol.*, vol. 5, Apr. 2014, Art. no. 296.
- [68] C. Basar-Eroglu et al., "P300-response: Possible psychophysiological correlates in delta and theta frequency channels. A review," *Int. J. Psychophysiol.*, vol. 13, no. 2, pp. 161–179, Sep. 1992.
- [69] G. Orellana and A. Slachevsky, "Executive functioning in schizophrenia," *Front. Psychiatry*, vol. 4, Jun. 2013, Art. no. 35.
- [70] M. Corbetta and G. L. Shulman, "Spatial neglect and attention networks," *Annu. Rev. Neurosci.*, vol. 34, pp. 569–599, Jul. 2011.
- [71] A. Suzuki et al., "A cortical cell ensemble in the posterior parietal cortex controls past experience-dependent memory updating," *Nature Commun.*, vol. 13, no. 1, Jan. 2022, Art. no. 41.
- [72] H. Tang et al., "Resting-state functional connectivity and deception: Exploring individualized deceptive propensity by machine learning," *Neuroscience*, vol. 395, pp. 101–112, Dec. 2018.
- [73] P. Molenberghs et al., "Understanding the minds of others: A neuroimaging meta-analysis," *Neurosci. Biobehavioral Rev.*, vol. 65, pp. 276–291, Jun. 2016.
- [74] M. Kireev et al., "Deceptive but not honest manipulative actions are associated with increased interaction between middle and inferior frontal gyri," *Front. Neurosci.*, vol. 11, Aug. 2017, Art. no. 482.
- [75] L. Fuentemilla et al., "Theta oscillations orchestrate medial temporal lobe and neocortex in remembering autobiographical memories," *NeuroImage*, vol. 85, pp. 730–737, Jan. 2014.
- [76] M. Kawasaki et al., "Fronto-parietal and fronto-temporal theta phase synchronization for visual and auditory-verbal working memory," *Front. Psychol.*, vol. 5, Mar. 2014, Art. no. 200.
- [77] D. Zhang et al., "Functional connectivity among multi-channel EEGs when working memory load reaches the capacity," *Brain Res.*, vol. 1631, pp. 101–112, Jan. 2016.
- [78] S. Haegens et al., " α -Oscillations in the monkey sensorimotor network influence discrimination performance by rhythmical inhibition of neuronal spiking," *Proc. Nat. Acad. Sci.*, vol. 108, no. 48, pp. 19377–19382, Nov. 2011.
- [79] R. D. Traub et al., "Layer 4 pyramidal neuron dendritic bursting underlies a post-stimulus visual cortical alpha rhythm," *Commun. Biol.*, vol. 3, no. 1, May 2020, Art. no. 230.
- [80] S. Haegens, L. Luther, and O. Jensen, "Somatosensory anticipatory alpha activity increases to suppress distracting input," *J. Cogn. Neurosci.*, vol. 24, no. 3, pp. 677–685, Mar. 2012.
- [81] C. Zhao et al., "Suppression of distracting inputs by visual-spatial cues is driven by anticipatory alpha activity," *PLoS Biol.*, vol. 21, no. 3, Mar. 2023, Art. no. e3002014.
- [82] D. D. Langleben et al., "Brain activity during simulated deception: An event-related functional magnetic resonance study," *NeuroImage*, vol. 15, no. 3, pp. 727–732, Mar. 2002.
- [83] Y. J. Zhou et al., "Alpha oscillations shape sensory representation and perceptual sensitivity," *J. Neurosci.*, vol. 41, no. 46, pp. 9581–9592, Nov. 2021.
- [84] D. Jokisch and O. Jensen, "Modulation of gamma and alpha activity during a working memory task engaging the dorsal or ventral stream," *J. Neurosci.*, vol. 27, no. 12, pp. 3244–3251, Mar. 2007.
- [85] S. Palva and J. M. Palva, "New vistas for α -frequency band oscillations," *Trends Neurosci.*, vol. 30, no. 4, pp. 150–158, Apr. 2007.
- [86] J. M. Palva, S. Palva, and K. Kaila, "Phase synchrony among neuronal oscillations in the human cortex," *J. Neurosci.*, vol. 25, no. 15, pp. 3962–3972, Apr. 2005.
- [87] Y. Wang et al., "Hierarchical neural prediction of interpersonal trust," *Neurosci. Bull.*, vol. 37, no. 4, pp. 511–522, Apr. 2021.
- [88] R. J. Huster et al., "Electroencephalography of response inhibition tasks: Functional networks and cognitive contributions," *Int. J. Psychophysiol.*, vol. 87, no. 3, pp. 217–233, Mar. 2013.
- [89] A. K. Engel and P. Fries, "Beta-band oscillations—Signalling the status quo?," *Curr. Opin. Neurobiol.*, vol. 20, no. 2, pp. 156–165, Apr. 2010.
- [90] M. Husain and P. Nachev, "Space and the parietal cortex," *Trends Cogn. Sci.*, vol. 11, no. 1, pp. 30–36, Jan. 2007.
- [91] M. Corbetta and G. L. Shulman, "Control of goal-directed and stimulus-driven attention in the brain," *Nature Rev. Neurosci.*, vol. 3, no. 3, pp. 201–215, Mar. 2002.
- [92] S. Treserras et al., "Transition from rest to movement: Brain correlates revealed by functional connectivity," *NeuroImage*, vol. 48, no. 1, pp. 207–216, Oct. 2009.